

Optical near-field enhancement by guided Bloch modes in plasmonic metasurfaces

Xiaorun Zang* and Andriy Shevchenko

Department of Applied Physics, Aalto University, P.O. Box 13500, FI-00076 Aalto, Finland

Local enhancement of light intensity by plasmonic nanostructures is essential for many optical applications, such as Surface-Enhanced Raman Spectroscopy (SERS) and fluorescence- or scattering-based plasmonic sensing. The enhancement is usually localized on the surface of each individual metal nanoparticle playing the role of a plasmonic resonator. In some cases, however, the particles are arranged in a periodic lattice and the excitations in them can be coupled to the surface lattice resonances (SLRs), which can additionally enhance the field. In this work, we report a field-enhancement mechanism that is based on the coupling between surface plasmon resonances in metal nanoparticles and Bloch modes guided by a dielectric-metal slab waveguide in a plasmonic metasurface. We demonstrate an extra factor of the local intensity enhancement of about 80 and the corresponding additional SERS enhancement of more than 6000 compared to isolated plasmonic nanoparticles on a thick glass substrate. This mechanism opens the possibility to design extraordinarily efficient metal-dielectric metasurfaces for many applications in optics and photonics, including SERS, fluorescence spectroscopy, nonlinear optics, and solar energy harvesting.

I. INTRODUCTION

Local enhancement of optical fields plays an essential role in many applications of optics and photonics, including optical sensors and detectors [1, 2], light sources [3? – 5], photovoltaic devices [6–8], and nonlinear optical components [9–13]. The enhancement can be achieved either inside or in the vicinity of an optical resonator. A particularly efficient near-field enhancement can be obtained with the help of metal nanostructures [14] that exhibit localized surface plasmon resonances (LSPRs) [15, 16]. The locations of abrupt and small-volume inhomogeneities of the structures, such as interparticle gaps and sharp edges, show highest field intensities. These "hot spots" look bright if the structure is used to locally enhance fluorescence or Raman scattering. The approach is especially important for Raman scattering, because this naturally off-resonant process has a small scattering cross section.

The near-field enhancement by plasmonic nanoparticles lies in the core of SERS [17, 18], which is a technique allowing identifying multiple molecular species in a single measurement with a single-wavelength excitation. The technique is free of photobleaching, which makes it advantageous over the fluorescence spectroscopy. However, a drawback of the technique is that naked metal nanostructures are not suitable for multiple use because of their fast and irreversible degradation caused, e.g., by humidity variations, surface oxidation, and contamination. The structures could be protected with a few-nm-thick dielectric coating, but this usually lowers the enhancement factor (η_{SERS}) by orders of magnitude.

Arrays of metal nanoparticles of various shapes and arrangements mounted on a dielectric substrate are called optical metasurfaces [19–21], if they are designed to control the macroscopic properties of light, such as its propagation direction, in an unconventional way. These struc-

tures can also be used to achieve a strong near-field enhancement, e.g., by making them impedance-matched to vacuum or a liquid analyte. This would improve trapping and enhancement of light on the surface. On the other hand, a metasurface can be made highly nonlocal [22] via coupling of the incident field to propagating surface modes, which can lead to a surface enhancement of the field as well [19].

In this paper, we explore the latter mechanism and show that the additional enhancement can be rather high, e.g., high enough to compensate for the decrease of η_{SERS} due to a protecting dielectric coating mentioned above. This makes it possible to create reusable SERS substrates with enhancement factors similar to those of ordinary unprotected substrates. We design a metasurface made of silver nanodimers periodically arranged on a dielectric-core slab waveguide. Besides a gap enhancement in each silver nanodimer, an additional enhancement arises from coupling of the incident light to guided Bloch modes. These modes belong to the second stop band of the structure, exhibiting a SLR at normal incidence. Metasurfaces of this type can be used not only for SERS [23], but also for many other spectroscopic applications. For the purpose of demonstration, we consider a SERS substrate operating at a wavelength of 780 nm, one of typical wavelengths in Raman spectroscopy. However, the approach can be used to enhance optical fields at other wavelengths too.

The paper is organized as follows. In Section II, we study the guided modes of a one-dimensional slab waveguide. This study provides a starting point for the design of a two-dimensional (2D) metasurface and a physical insight into the properties of possible guided Bloch modes. In Section III, we establish a connection between the near-field enhancement spectra in a designed 2D metasurface and the empty-lattice Bloch-mode band diagrams. In Section IV, we optimize the designed metasurface to maximize its near-field enhancement factor. To achieve a significant additional enhancement of light in the gap hot spots, we match the frequencies of the SLRs

* xiaorun.zang@aalto.fi

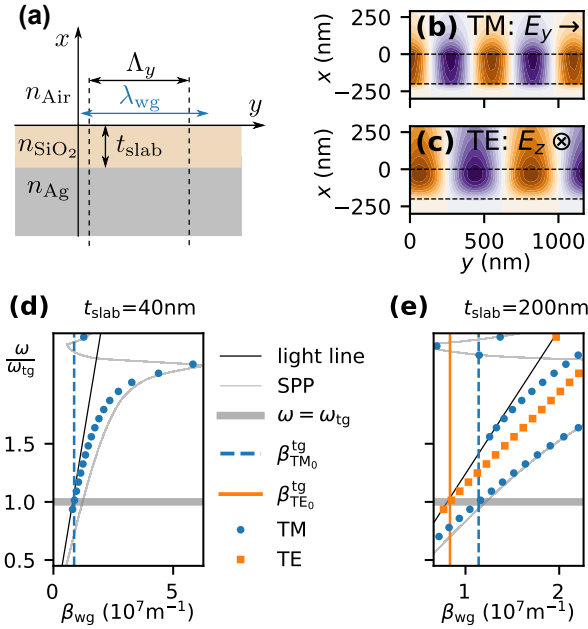


Figure 1. (a) A schematic diagram of a silver-silica-air slab waveguide. Field profiles of the fundamental (b) TM and (c) TE modes when the slab thickness is $t_{\text{slab}} = 200$ nm. The dispersion curves are plotted for (d) $t_{\text{slab}} = 40$ nm and (e) $t_{\text{slab}} = 200$ nm.

and the guided modes by varying the lattice periods and slab thickness. The conclusions are drawn in Section V.

II. GUIDED MODES IN A SLAB WAVEGUIDE

A metasurface considered in this work is composed of a slab waveguide and a lattice of nanoparticles (meta-atoms) on its surface. We first study the properties of the waveguide alone, treating it as a periodic structure with an empty lattice of meta-atoms [19, 24]. A group of qualitatively similar dispersion relations can then be found in a metasurface based on the same slab waveguide [24, 25]. Therefore, it is useful to first investigate the modal dispersion of a slab waveguide and then apply the obtained knowledge to the problem of the near-field enhancement in a real 2D metasurface.

The waveguide is made of a silica slab on a silver substrate [see Fig. 1(a)]. The silver substrate can also enhance the field on the surface by simply reflecting the incident field. The refractive indices of silver, silica, and air are denoted by n_{Ag} , n_{SiO_2} , and n_{air} , respectively. The field profiles of the fundamental TM and TE modes are shown in Figs. 1(b) and 1(c), respectively, for a slab thickness of $t_{\text{slab}} = 200$ nm at the wavelength of 780 nm. The TM mode has a dominant field component E_y due to the presence of silver at the bottom of the waveguide. It is more concentrated inside the slab and resembles a surface plasmon polariton (SPP) mode at a silver-silica interface. However, the TE mode has only the E_z com-

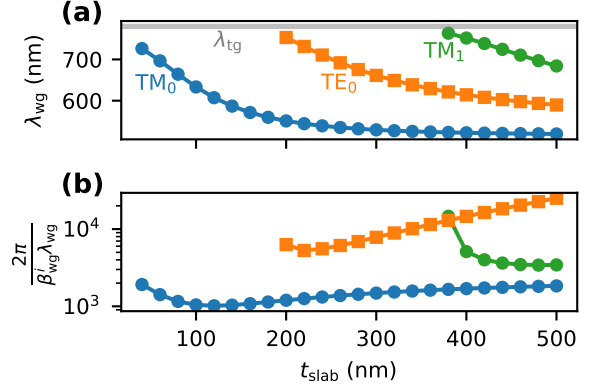


Figure 2. (a) Mode wavelengths $\lambda_{\text{wg}} = 2\pi/\beta_{\text{wg}}^r$ of the slab waveguide; (b) Normalized decay lengths $2\pi/\beta_{\text{wg}}^i/\lambda_{\text{wg}}$ for varying slab thickness.

ponent that is nearly negligible at the metal surface and have intensity maxima closer to the silica-air interface. In addition, the TM mode has a shorter modal wavelength than the TE mode, with the former being $\lambda_{\text{TM}_0} = 550$ nm and the latter being $\lambda_{\text{TE}_0} = 780$ nm. The modal dispersion curves of slab waveguides with $t_{\text{slab}} = 40$ nm and $t_{\text{slab}} = 200$ nm are plotted in Figs. 1(d) and 1(e), respectively. For relatively thin slabs, the fundamental TM mode approximately follows the dispersion curve of the SPP on a silver-silica interface at high frequencies, while it approaches the light line in air at low frequencies. If the slab thickness increases, more modes emerge and the dispersion curve of the fundamental TM mode is pushed towards the SPP curve. The target wavelength of 780 nm is shown by the horizontal solid grey line that intersects with the dispersion curves and determines the modal propagation constants $\beta_{\text{TM}_0}^{\text{tg}}$ and $\beta_{\text{TE}_0}^{\text{tg}}$ at this wavelength.

The wavelengths of the guided modes, $\lambda_{\text{wg}} = 2\pi/\beta_{\text{wg}}^r$, with β_{wg}^r denoting the real part of the propagation constant, are shown in Fig. 2(a) for varying slab thicknesses. In addition, the normalized decay lengths, $2\pi/\beta_{\text{wg}}^i/\lambda_{\text{wg}}$ [26], are plotted in Fig. 2(b), where β_{wg}^i is the imaginary part of the propagation constant. The guided modes can therefore propagate over a distance of $10^3 - 10^4$ modal wavelengths, leading to a long-distance, highly nonlocal interaction of the meta-atoms.

III. BLOCH MODES IN PLASMONIC METASURFACES

Before discussing the guided Bloch modes and SLRs in our designed metasurfaces, we extend the empty-lattice dispersion relation of the free-photon approximation [19, 24] to the free-guided-wave approximation. The empty-lattice dispersion relation is

$$|\mathbf{k}_{\parallel} + \mathbf{G}| = \beta_{\text{wg}}, \quad (1)$$

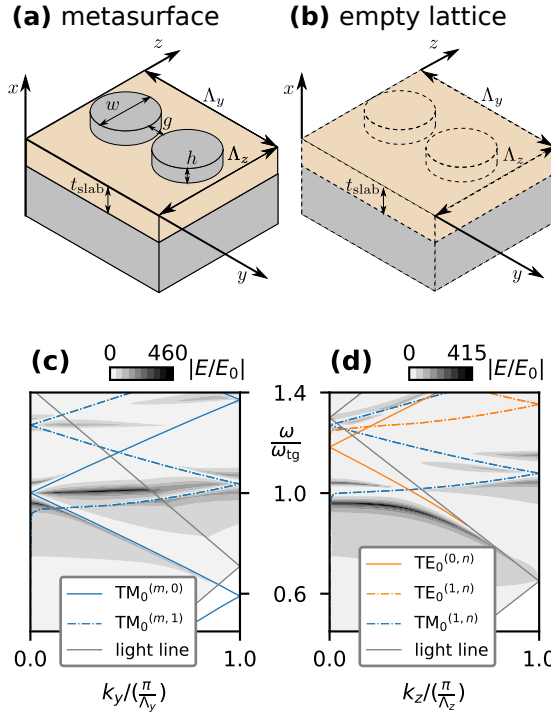


Figure 3. Schematic diagrams of (a) a metal-dielectric metasurface and (b) the corresponding empty lattice. The parameter values used in the calculations are $\Lambda_y = 550$ nm, $\Lambda_z = 600$ nm, and $t_{\text{slab}} = 200$ nm. The near-field enhancement in the metasurface and the empty-lattice dispersion curves are shown in (c) and (d).

where $\mathbf{k}_{||} = \hat{y}k_y + \hat{z}k_z$ is the in-plane Bloch wave vector, $\mathbf{G} = m\frac{2\pi}{\Lambda_y} + n\frac{2\pi}{\Lambda_z}$ is the reciprocal lattice vector (with the integers m and n denoting the Bloch-mode orders along the y and z directions, respectively), and β_{wg} is the propagation constant of the slab mode. The slab waveguide is homogeneous and extends to infinity in the transverse plane. However, the fictitious periodicity causes the band folding [19, 24, 25, 27]. If we choose the periods to be equal to the guided-mode wavelengths, the empty-lattice Bloch modes could be excited at normal incidence [27], corresponding to the Γ -point.

In a metasurface containing silver meta-atoms, the meta-atomic LSPRs are coupled to the empty-lattice Bloch modes, resulting in modified Bloch modes [19]. The unit cell of the metasurface is shown in Fig. 3(a). It contains a meta-atom in the form of a silver-disc dimer with dimensions $w = 120$ nm, $h = 20$ nm, and $g = 6$ nm. The values of other parameters of the structure are $t_{\text{slab}} = 200$ nm, $\Lambda_y = 550$ nm, and $\Lambda_z = 600$ nm. At $\lambda = 780$ nm, the period Λ_y is equal to the mode wavelength λ_{TM_0} , but the period Λ_z is shorter than λ_{TE_0} . Note that plasmonic dimers are among the most efficient standard nanoparticles used to locally enhance optical fields.

A p -polarized incident plane wave (with the electric field lying in the xy -plane) couples effectively to the TM

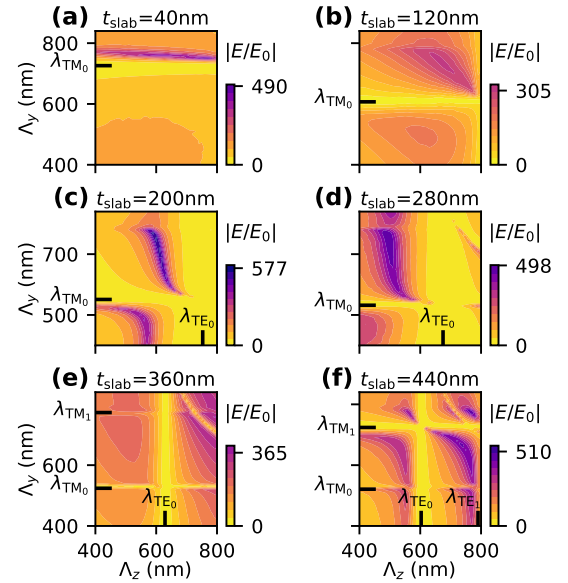


Figure 4. Near-field enhancement factor $|E/E_0|$ as a function of periods Λ_y and Λ_z for several slab thicknesses t_{slab} at wavelength $\lambda_{\text{tg}} = 780$ nm. Thick black ticks with labels λ_{TM_0} , λ_{TM_1} , and λ_{TE_0} mark the guided-mode wavelengths.

Bloch modes of the structure, yielding Fano-type [28] asymmetric line shapes in the near-field enhancement spectra. This is revealed in Fig. 3(c), where high (in black) and low (in white) near-field enhancement factors appear near the empty-lattice dispersion curves. A band gap is formed at the normalized frequency $\omega/\omega_{\text{tg}} = 1$ at $k_y = 0$, as a result of coupling of the LSPR with the empty-lattice Bloch modes $\text{TM}_0^{(+1,0)}$ and $\text{TM}_0^{(-1,0)}$ that counter-propagate along axis y . For higher-order empty-lattice TM modes with order $n = 1$ (the blue dashed curve), another band gap is formed near the normalized frequency $\omega/\omega_{\text{tg}} = 1.04$ at $k_y = \pi/\Lambda_y$.

If light is incident in the zx -plane and s -polarized, it couples effectively to the Bloch modes propagating in the z -direction. The excited LSPRs in the dimers still provide a high gap enhancement. In Fig. 3(d), one can observe band gaps at $\omega/\omega_{\text{tg}} = 1.0$ and 1.08 due to the interaction of LSPRs with the $\text{TM}_0^{(1,n)}$ modes at $k_z = 0$ and $k_z = \pi/\Lambda_z$, respectively. The interaction leads to high near-field enhancement factors (see the dark regions in the figure). Additional empty-lattice TE and TM modes do not significantly affect the near-field enhancement and they are not shown in the figure.

IV. NEAR-FIELD ENHANCEMENT IN A 2D METASURFACE

We can now maximize the near-field enhancement by optimizing the periods Λ_y and Λ_z , as well as the slab

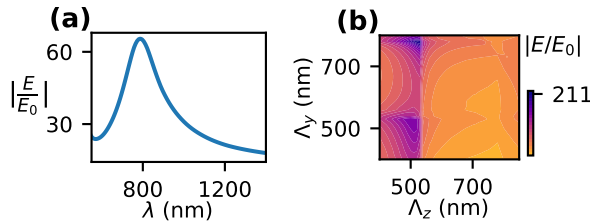


Figure 5. Near-field enhancement factors of (a) a single dimer and (b) a lattice of dimers on top of a semi-infinite silica.

thickness t_{slab} . As shown in Fig. 4(a-f), both the periods affect the near-field enhancement, and the fingerprints of band gaps are recognized as straight stripes of low near-field enhancement near the periods equal to the guided-mode wavelengths (indicated by thick black ticks with labels λ_{TM_0} , λ_{TM_1} , and λ_{TE_0}). The Bloch modes formed above or below the guided-mode wavelengths contribute the most to the near-field enhancement in the gaps of the nanoparticles. A maximum field enhancement, $|E/E_0| = 577$, is achieved at periods $\Lambda_z = 595$ nm and $\Lambda_y = 760$ nm for the slab thickness $t_{\text{slab}} = 200$ nm. Such a configuration allows for a SERS enhancement factor, η_{SERS} , of the order of 10^{11} at a gap size of 6 nm. At smaller gaps, the enhancement factor is larger, but we consider 6 nm as a reasonable gap size that can be obtained in nanofabricated samples.

It is interesting to compare the near-field enhancement in the optimized metasurface to that of a single dimer and a lattice of dimers on a thick silica substrate. For an isolated single dimer on a thick substrate, the near field can be resonantly enhanced by a factor of 65 at $\lambda = 780$ nm, as shown in Fig. 5(a). If such dimers are arranged periodically in a lattice on the same substrate, an extra factor of 3 can be obtained for the near-field enhancement [see Fig. 5(b)]. In our design, with a silver mirror positioned at a distance of 200 nm below the surface, an overall near-field enhancement of 577 is obtained. Hence, arranging the particles in a lattice on a slab waveguide resulted in about 80 times higher local-field intensity in the gaps compared to the case of isolated dimers on a thick substrate, providing an extra SERS enhancement of more than 6000 (calculated as a squared intensity enhancement). This is a significant number. The extra enhancement can for example compensate for a decrease of SERS signal by a protecting dielectric layer needed to make the substrates reusable.

We further explore the near-field enhancement spectra of three designed metasurfaces with $t_{\text{slab}} = 200$ nm, marked by points D, E, and F in Fig. 6(a)-(c). For the metasurface at point D, the periods are $\Lambda_y = 550$ nm and $\Lambda_z = 595$ nm, and the near-field enhancement is very low due to the band gap at the normalized frequency

$\omega/\omega_{\text{tg}} = 1$ at $k_y = 0$ [see Fig. 6(d)]. This band gap is formed because the period Λ_y matches with the modal wavelength $\lambda_{\text{TM}_0} = 550$ nm of the fundamental TM mode propagating along the y axis [see Fig. 2(a)].

At point E, the periods are $\Lambda_y = 760$ nm and $\Lambda_z = 755$ nm, with the latter being close to the modal wavelength $\lambda_{\text{TE}_0} = 753$ nm of the fundamental TE mode propagating along the z axis [see Fig. 2(a)]. This results in a band gap at the normalized frequency $\omega/\omega_{\text{tg}} = 1$ at $k_z = 0$ [see Fig. 6(e)], which makes the near-field enhancement low.

The maximum near-field enhancement is obtained for the metasurface at point F with a pair of periods $\Lambda_y = 760$ nm and $\Lambda_z = 595$ nm. As shown in Fig. 6(f), the upper band of the guided Bloch mode is formed at the normalized frequency $\omega/\omega_{\text{tg}} = 1$ at $k_y = 0$, because Λ_y is larger than the modal wavelength λ_{TM_0} . On the other hand, the lower band of the guided Bloch mode is formed at the normalized frequency $\omega/\omega_{\text{tg}} = 1$ at $k_z = 0$, as Λ_z is smaller than the modal wavelength λ_{TE_0} . The upper and lower bands of the guided Bloch modes counter-propagating along the y and z axes jointly enhance the near-field in the gaps of the dimers.

V. CONCLUSIONS

We have shown that, with the aid of guided Bloch modes in a designed nonlocal optical metasurface, the local SERS enhancement can be increased by orders of magnitude in addition to the standard enhancement by plasmonic nanoparticles. The additional enhancement mechanism relies on coupling of the incident light to the Bloch modes guided along the surface in a metal-dielectric slab waveguide. The coupling takes place at the second stop band. The maximum enhancement is obtained by optimizing the two periods and the thickness of the waveguide. For plasmonic nanoparticles forming dimers, we predict an overall SERS enhancement of 10^{11} at a gap size of 6 nm between the particles. By reducing the gap, the enhancement factor can be further increased. We expect that the proposed mechanism of additional near-field enhancement will find applications not only in SERS, but also in fluorescence- and scattering-based plasmonic sensing, light-energy harvesting components, and nonlinear optics.

ACKNOWLEDGMENTS

We acknowledge the Academy of Finland Flagship Programme Photonics Research and Innovation (PREIN; grant No. 320167). We thank Dr. R. Kolkowski for fruitful discussions and advice on theoretical simulations of metasurfaces and slab waveguide modes. We also acknowledge the computational resources provided by the Aalto Science-IT project.

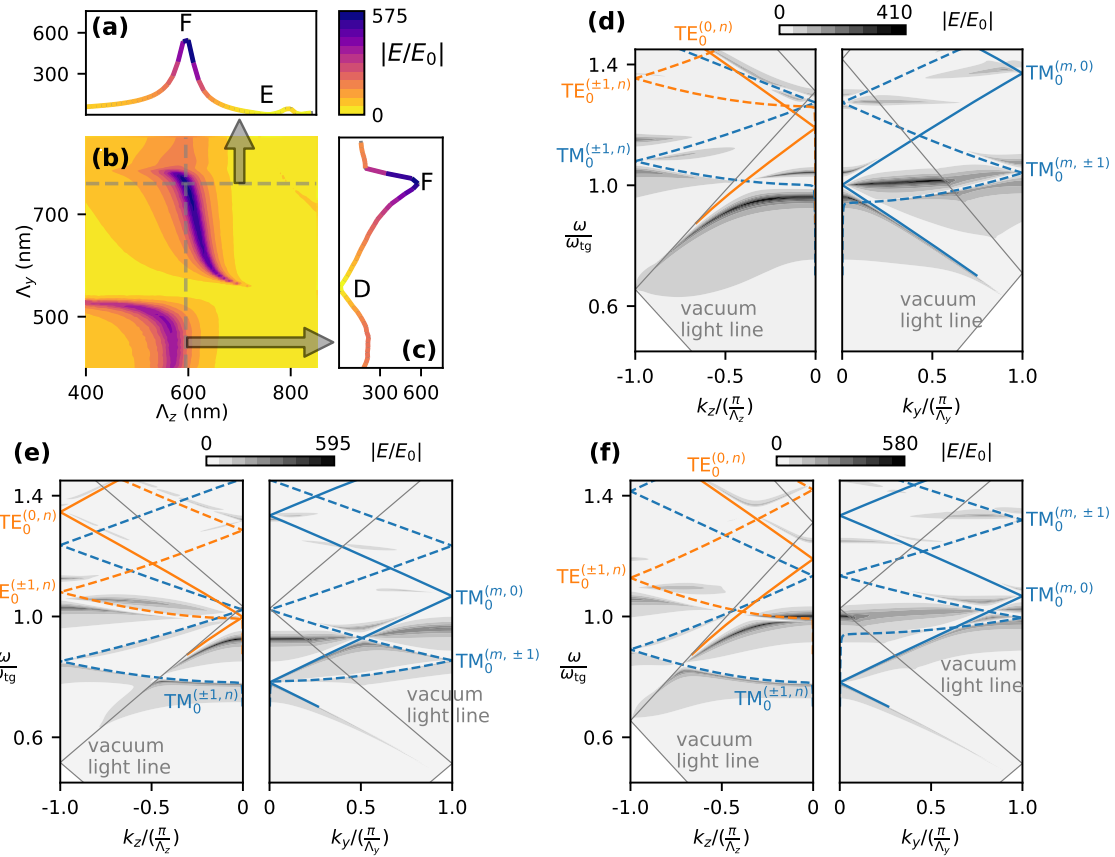


Figure 6. Near-field enhancement spectra for $t_{\text{slab}} = 200$ nm and (a) a fixed period $\Lambda_y = 760$ nm, (b) varying periods Λ_y and Λ_z , and (c) a fixed period $\Lambda_z = 595$ nm. For three typical configurations a points D, E, and F, the near-field enhancement spectra as a function of the incidence angles along the y and z axes are shown in (d), (e), and (f), respectively. Blue and orange lines indicate the empty-lattice Bloch modes $\text{TM}_0^{(m,n)}$ and $\text{TE}_0^{(m,n)}$, respectively. In both colors, solid lines indicate the zero-order modes, whereas the dashed lines stand for the 1st-order modes.

[1] B. Liedberg, C. Nylander, and I. Lunström, Surface plasmon resonance for gas detection and biosensing, *Sensors and Actuators* **4**, 299 (1983).

[2] J. Homola, S. S. Yee, and G. Gauglitz, Surface plasmon resonance sensors: Review, *Sensors and Actuators B: Chemical* **54**, 3 (1999).

[3] R. F. Oulton, V. J. Sorger, T. Zentgraf, R.-M. Ma, C. Gladden, L. Dai, G. Bartal, and X. Zhang, Plasmon lasers at deep subwavelength scale, *Nature* **461**, 629 (2009).

[4] R. F. Oulton, Surface plasmon lasers: Sources of nanoscopic light, *Materials Today* **15**, 26 (2012).

[5] Y. Liang, C. Li, Y.-Z. Huang, and Q. Zhang, Plasmonic nanolasers in on-chip light sources: Prospects and challenges, *ACS Nano* **14**, 14375 (2020).

[6] D. M. Schaad, B. Feng, and E. T. Yu, Enhanced semiconductor optical absorption via surface plasmon excitation in metal nanoparticles, *Applied Physics Letters* **86**, 063106 (2005).

[7] S. Pillai and M. A. Green, Plasmonics for photovoltaic applications, *Solar Energy Materials and Solar Cells* **94**, 1481 (2010).

[8] H. A. Atwater and A. Polman, Plasmonics for improved photovoltaic devices, *Nature Materials* **9**, 205 (2010).

[9] A. Bouhelier, M. Beversluis, A. Hartschuh, and L. Novotny, Near-field second-harmonic generation induced by local field enhancement, *Physical Review Letters* **90**, 013903 (2003).

[10] M. Kauranen and A. V. Zayats, Nonlinear plasmonics, *Nature Photonics* **6**, 737 (2012).

[11] J. Berthelot, G. Bachelier, M. Song, P. Rai, G. C. des Francs, A. Dereux, and A. Bouhelier, Silencing and enhancement of second-harmonic generation in optical gap antennas, *Optics Express* **20**, 10498 (2012).

[12] B. Metzger, L. Gui, J. Fuchs, D. Floess, M. Hentschel, and H. Giessen, Strong enhancement of second harmonic emission by plasmonic resonances at the second harmonic wavelength, *Nano Letters* **15**, 3917 (2015).

[13] R. Czaplicki, A. Kiviniemi, M. J. Huttunen, X. Zang, T. Stolt, I. Vartiainen, J. Butet, M. Kuittinen, O. J. F. Martin, and M. Kauranen, Less is more: Enhancement of second-harmonic generation from metasurfaces by reduced nanoparticle density, *Nano Letters* **18**, 7709 (2018).

[14] C. Ciraci, R. T. Hill, J. J. Mock, Y. Urzhumov, A. I. Fernández-Domínguez, S. A. Maier, J. B. Pendry, A. Chilkoti, and D. R. Smith, Probing the ultimate limits of plasmonic enhancement, *Science* **337**, 1072 (2012).

[15] T. Klar, M. Perner, S. Grosse, G. von Plessen, W. Spirk, and J. Feldmann, Surface-plasmon resonances in single metallic nanoparticles, *Physical Review Letters* **80**, 4249 (1998).

[16] S. A. Maier, *Plasmonics: Fundamentals and Applications* (Springer, New York, 2007).

[17] S. Nie and S. R. Emory, Probing single molecules and single nanoparticles by surface-enhanced Raman scattering, *Science* **275**, 1102 (1997).

[18] K. Kneipp, M. Moskovits, and H. Kneipp, *Surface-Enhanced Raman Scattering: Physics and Applications* (Springer, Berlin; New York, 2006).

[19] C. Cherqui, M. R. Bourgeois, D. Wang, and G. C. Schatz, Plasmonic surface lattice resonances: Theory and computation, *Accounts of Chemical Research* **52**, 2548 (2019).

[20] I. Radko, V. Volkov, J. Beermann, A. Evlyukhin, T. Søndergaard, A. Boltasseva, and S. Bozhevolnyi, Plasmonic metasurfaces for waveguiding and field enhancement, *Laser & Photonics Reviews* **3**, 575 (2009).

[21] S. Gwo, C.-Y. Wang, H.-Y. Chen, M.-H. Lin, L. Sun, X. Li, W.-L. Chen, Y.-M. Chang, and H. Ahn, Plasmonic metasurfaces for nonlinear optics and quantitative SERS, ACS Photonics **3**, 1371 (2016).

[22] A. Overvig and A. Alù, Diffractive nonlocal metasurfaces, *Laser & Photonics Reviews* **16**, 2100633 (2022).

[23] A. Shevchenko, V. Ovchinnikov, and A. Shevchenko, Large-area nanostructured substrates for surface enhanced Raman spectroscopy, *Applied Physics Letters* **100**, 171913 (2012).

[24] K. T. Carron, W. Fluhr, M. Meier, A. Wokaun, and H. W. Lehmann, Resonances of two-dimensional particle gratings in surface-enhanced Raman scattering, *Journal of the Optical Society of America B* **3**, 430 (1986).

[25] S. G. Tikhodeev, A. L. Yablonskii, E. A. Muljarov, N. A. Gippius, and T. Ishihara, Quasiguided modes and optical properties of photonic crystal slabs, *Physical Review B* **66**, 045102 (2002).

[26] L. Solymar and E. Shamonina, *Waves in Metamaterials* (Oxford University Press, Oxford ; New York, 2009).

[27] V. Yannopapas and N. Stefanou, Optical excitation of coupled waveguide-particle plasmon modes: A theoretical analysis, *Physical Review B* **69**, 012408 (2004).

[28] D. Khlopin, F. Laux, W. P. Wardley, J. Martin, G. A. Wurtz, J. Plain, N. Bonod, A. V. Zayats, W. Dickson, and D. Gérard, Lattice modes and plasmonic linewidth engineering in gold and aluminum nanoparticle arrays, *Journal of the Optical Society of America B* **34**, 691 (2017).